Journal of
Stem Cell Research & Therapy
ISSN: 2157-7633

Oh et al., J Stem Cell Res Ther 2016, 6:1
DOI: 10.4172/2157-7633.1000323

Research Article Open Access

Protective Effect of S-Adenosyl-L-Methionine on Oxidative Stress-Induced Apoptosis Regulates Nrf2 via IGF-I in Rat Bone Marrow Mesenchymal Stem Cells

Myung-Hoon Oh, Jong-Hoon Kim and Chang-Won Kang*

Department of Veterinary Physiology, College of Veterinary Medicine/ Bio-Safety Research Institute, Chonbuk National University, South Korea

Abstract

Bone marrow mesenchymal stem cell (MSC)-mediated regeneration is a promising treatment for degenerative diseases and traumatic injuries. S-Adenosyl-L-methionine (SAM) is the principal biological methyl donor. We hypothesized that the cytoprotective effect of SAM on oxidative stress-induced apoptosis in rat MSCs is due to insulin-like growth factor-I (IGF-I) and nuclear factor erythroid 2-related factor 2 (Nrf2). SAM (10 μM) increased both endogenous IGF-I levels and cell viability ($p<0.05$). In MSCs, 1 mM H_2O_2 at 6 h significantly decreased cell viability and IGF-I and Nrf2 activation, but increased ROS generation ($p<0.05$ and $p<0.01$, respectively). The decrease in cell viability, endogenous IGF-1, and Nrf2 in H_2O_2-induced apoptosis was recovered by SAM (10 μM). Apoptosis induced by H_2O_2 also decreased Nrf2 activity, as determined by immunofluorescence staining, but the decrease was also recovered by SAM. We demonstrated that H_2O_2-induced apoptosis was reduced by SAM through Annexin-V. Using a specific small interfering RNA (siRNA), the increase in SAM-induced cell viability and endogenous Nrf2 in the presence of H_2O_2 was suppressed by IGF-I siRNA, but the endogenous IGF-I level was not changed by Nrf2 siRNA. The increase in endogenous Nrf2 with exogenous IGF-I and H_2O_2 treatment was also suppressed by Nrf2 siRNA, but the IGF-I level was not inhibited ($p<0.05$). These results suggest that the cytoprotective effect of SAM against H_2O_2-induced apoptosis is mediated by increased Nrf2 activity through IGF-I. These factors could regulate the metabolic fate and survival of MSCs.

Keywords: Insulin-like growth factor-I; Nuclear factor erythroid 2-related factor 2; Oxidative stress; Apoptosis; Mesenchymal stem cells

Abbreviations: IGF-I: Insulin-like Growth Factor-I; MSC: Bone marrow Mesenchymal Stem Cell; Nrf2: Nuclear Factor Erythroid 2-related Factor 2; SAM: S-adenosyl-L-methionine; H_2O_2: Hydrogen peroxide.

Introduction

Mesenchymal stem cells (MSCs) can differentiate into osteoblasts, chondroblasts, adipocytes, pancreatic cells, and other functional cells under appropriate cell culture conditions [1,2]. This multipotent differentiation potential defines MSCs, and studies have suggested their many possible therapeutic applications [3,4]. For example, the transplantation of MSCs is an effective treatment for tissue injuries including myocardial infarction, hind limb ischemia, acute renal failure, and liver transplantation [5,6]. Despite the advantages of MSCs, they have not shown satisfactory effects in some studies, mostly due to poor survival after transplantation [7,8]. Inflammation, chemotherapy, radiotherapy, and pro-apoptotic factors in the microenvironment of the damaged tissue do not favor MSC survival. In addition, the generation and maintenance of high levels of reactive oxidative species (ROS) are seen in CNS diseases, which promote cellular apoptosis [9]. Hence, MSCs must be reinforced to withstand these stresses before they can function as effective therapies. The exact cellular mechanisms resulting in the survival-promoting effects of MSCs loss are not clear [10,11]. Therefore, in this study, we investigated the cytoprotective effects of SAM on oxidative stress-induced apoptosis in rat MSCs through its effects on insulin-like growth factor-I (IGF-I) and nuclear factor erythroid 2-related factor 2 (Nrf2).

S-Adenosyl-L-methionine (SAM) is the principal biological methyl donor and is the precursor of the aminopropyl groups used in polyamine biosynthesis. SAM is also important for nucleic acid metabolism and regulation, as well as for the structure and function of membranes and other cellular constituents [12,13]. SAM is particularly important for reducing free radical toxicity from various toxins [14]. The cytoprotective effect of SAM is well-known [15,16]. However, the cytoprotective effect of SAM on oxidative stress-induced apoptosis has not been studied in murine MSCs.

Insulin-like growth factor-I (IGF-I) (a mitogenic and anti-apoptotic peptide) is a growth hormone that plays an important role in bone cell proliferation and apoptosis [17,18]. Furthermore, IGF-I is a potent anabolic growth factor and anti-oxidative hormone [19,20].

Nuclear factor erythroid 2-related factor 2 (Nrf2) is a basic leucine zipper transcription factor that binds to and activates anti-oxidative response elements (AREs) [21-23]. Nrf2 is critical for protecting against electrophilic and oxidative stress [24,25]. *In vitro*, Nrf2 has been shown to be phosphorylated at Ser40 by protein kinase C [26]. Activated Nrf2 impairs liver regeneration in mice by activating genes involved in cell-cycle control and apoptosis [27]. Many antioxidant- and detoxification-related gene promoters, such as glutathione transferases, HO-1, superoxidant dismutant, and thioredoxin, contain ARE [28]. Activation of the Nrf2 transcription factor has been linked to cytoprotection [22,23]. However, the relationship between SAM and

***Corresponding author:** Chang-Won Kang, Department of Veterinary Physiology, College of Veterinary Medicine, Chonbuk National University, Kobong-ro 79, Iksan -si, Chonbuk, South Korea, Tel: + 82 63 850 0937; E-mail: cwkang@jbnu.ac.kr

Received January 06, 2016; **Accepted** January 19, 2016; **Published** January 26, 2016

Citation: Oh MH, Kim JH, Kang CW (2016) Protective Effect of S-Adenosyl-L-Methionine on Oxidative Stress-Induced Apoptosis Regulates Nrf2 via IGF-I in Rat Bone Marrow Mesenchymal Stem Cells. J Stem Cell Res Ther 6: 323. doi:10.4172/2157-7633.1000323

endogenous Nrf2 and IGF-I in preventing oxidative stress is unclear in rat MSCs. Therefore, this study investigated effects of SAM on the expression of endogenous IGF-I and Nrf2 in murine MSCs in the setting of oxidative stress. Our results can provide important insights into methods for increasing MSC stability in order to improve the efficacy of mesenchymal stem cell therapy for oxidative stress-induced apoptosis.

Materials and Methods

Primary culture (MSC extraction and culture)

MSCs were isolated from long bones (femur and tibia) of 4-to-5-week-old male Sprague-Dawley rats and cultured using a modification of a previously described method [29]. Briefly, mononuclear cells were isolated from bone marrow using density gradient centrifugation (1600 rpm for 30 min) with Ficoll-Paque™ plus (GE Healthcare Science, Buckinghamshire, UK). Isolated cells were sorted using magnetic-activated cell sorting (MACS) with a specific antibody (CD105-positive selection). The cells were plated in a T-75 flask with basal culture medium (Dulbecco's Modified Eagle Medium, DMEM), 10% FBS, 2 mM L-glutamine, 100 IU/mL penicillin, and 100 mg/mL streptomycin in a humidified atmosphere at 37°C with 5% CO_2. MACS is the trademarked name for a method to separate various cell populations on the basis of surface antigens (CD molecules). A mixture of cells to be separated is incubated with magnetic beads coated with antibodies against a particular surface antigen. Cells expressing the antigen attach to the magnetic beads, and the solution is transferred to a column within a strong magnetic field. The cells attached to the beads (those expressing the antigen) remain on the column, while the other cells (not expressing the antigen) flow through. This method can select and isolate cells positive for CD105 from a mixed population of cells. Fluorescence-activated cell sorting (FACS) analysis was performed as described previously [30]. After 10 min of incubation with a specific antibody, the samples were diluted 1:5 in buffer and measured with flow cytometric analysis using a FACSCalibur apparatus (Becton Dickinson, Piscataway, NJ, USA).

Cell transfection and small interfering RNA (siRNA)

siRNAs targeting IGF-I were synthesized by Integrated DNA Technology (Santa Cruz Biotechnology, Santa Cruz, CA, USA). Adherent MSCs were incubated overnight in the aforementioned medium containing 10% FBS until they were 80% confluent. Cells were transfected with 10 nM siRNAs using Lipofectamine 2000 (Life Technology, Carlsbad, CA, USA) according to the manufacturer's instructions. The mixture was incubated for 30 min to form a siRNA-lipid complex, and the cells were added to the mixture. After incubating for 6 h, cells were incubated with or without additional treatments in medium containing 0.2% BSA for 24 h. Finally, target gene expression was assayed using scrambled siRNA as a negative control.

Immunocytochemistry

For immunostaining, cells fixed with 4% paraformaldehyde were washed three times with phosphate-buffered saline (PBS) and permeabilized with 0.3% Triton X-100 and 0.2% bovine serum albumin for 10 min. Cells were washed with PBS and incubated with the monoclonal mouse Nrf2 antibody (1:200) for 2 h at room temperature. The cells were incubated with a FITC-conjugated secondary antibody (1:500) for 1 h at room temperature. Finally, cells were washed three times with PBS (10 min each) and observed under an EVOS microscope (Thermo Fisher Scientific, Waltham, MA, USA).

Immunoprecipitation and western blotting

Isolated cells were incubated in Triton X-100 lysis buffer at 4°C for 30 min in an orbital shaker. To remove insoluble material, the lysate was centrifuged at 14,000 rpm for 5 min at 4°C. Supernatants were precleared by adding 50 µl of 20% pansorbin (Calbiochem, San Diego, CA, USA) to each sample and incubating for 1 h at 4°C. Aliquots of supernatant containing equal amounts of protein were immunoprecipitated for 2 h at 4°C with either anti-IGF-I Ab/rabbit anti-mouse lgG (Gropep Bioreagents, Thebarton, SA, Australia), protein A-Sepharose (Pharmacia LKB Biotechnology AB, Uppsala, Sweden) conjugate, or anti-phosphotyrosine Ab-1 agarose conjugate. The pellet was dissolved in a sample buffer for SDS–PAGE, heated for 10 min at 95°C, and analyzed using Western blot. Approximately 20-40 µg of each protein sample was subjected to 12% SDS-polyacrylamide gel electrophoresis (SDS-PAGE), and the resolved proteins were transferred to a PVDF membrane. The membrane was washed with phosphate-buffered saline (PBS) containing Tween-20 (PBS-T) and blocked with PBS containing 5% skim milk for 2 h at room temperature. The blots were incubated with specific antibodies against IGF-I, Nrf2, and β-actin (diluted to 1:1000) overnight at 4°C, followed by incubation with anti-rabbit horseradish peroxidase-conjugated secondary antibodies diluted to 1:3000. After washing, the specific protein bands were visualized with an enhanced chemiluminescence detection system (Santa Cruz Biotechnology, Santa Cruz, CA, USA). Band intensities were quantified with densitometric analysis using Alpha Imager Software (Alpha Innotech, San Leandro, CA, USA).

Reverse transcriptase-polymerase chain reaction (quantitative real-time PCR)

RNA was extracted from the cells with TRIzol reagent (Invitrogen, Carlsbad, CA, USA) according to the manufacturer's protocol. Three micrograms of total RNA was incubated at 60°C for 10 min, and a mixture containing 2 µl of 5X first-strand buffer, 1 µl of 0.1 M dithiothreitol (DTT), 1 µl of 10 mM dNTPs, 0.1 µg of random primer mix, RNase inhibitor, and M-MLV-reverse transcriptase (Invitrogen) was added. Samples were then incubated at 42°C for 60 min. Second-strand cDNA synthesis was conducted by combining 2 µl of each sample with 10 µl of SYBR Green qPCR Master mix and 0.1µM primer (IGF-I sense, 5'-CACAGGGTATGGCTC-3'; IGF-I antisense, 5'-CTTCTGGGTCTTGGG-3'; Nrf2 sense, 5′-GGGAGGTGGATGTAATGTGG-3′; Nrf2 antisense, 5′-TGGGCCTGGAACTACAACTC-3′). Water was added to a final volume of 20 µl. PCR was performed under the following conditions: 1 cycle of 95°C for 2 min, 40 cycles of 95°C for 15 sec, and annealing at 61°C for 30 sec. The DNA binding dye SYBR Green I incorporated into the double-stranded DNA during PCR amplification fluoresces at increasing intensity with each cycle. After 40 cycles, the products were quantified with the real-time PCR melting curve program (65°C - 95°C with a heating rate of 0.1°C/s and continuous fluorescence measurements) and cooling to 15°C. Glyceraldehyde-3-phosphate dehydrogenase (GAPDH) was used as a control.

Measurement of ROS

5-(and 6) Chloromethyl-2',7'-dichlorodihydrofluorescein diacetate acethyl ester (DCFH-DA) was used to measure ROS, as previously described [31]. Cells were harvested by centrifugation, washed twice with phosphate buffered saline (PBS), and suspended in PBS (1 × 106 cells/ml). 500 ml of cell suspension was placed in a polyethylene tube, incubated in PBS containing DCFH-DA (5 mM) for 15 min in a light-protected humidified chamber at 37°C, and were then rinsed in PBS.

For the DCFH-DA assay, excitation was at 488 nm with an emission at 540 nm. The fluorescence image was collected using a single rapid scan with identical parameters for all samples and was measured with a Fluorescence Microplate Reader (BioTek, Winooski, VT, USA). Fluorescence levels are expressed as the percent increase over the control. Experiments were performed in triplicate.

Cell lysis

The cells were rinsed twice with cold PBS and lysed in 20 mM HEPES, pH 8.8, 136 mM NaCl, 1 mM EDTA, 1 mM EGTA, 10 g/ml Triton X-100, 10 mM KCl, 2 mM MgCl, 1 mM phenylmethanesulfonyl fluoride (PMSF), 1 mM sodium orthovanadate, 1 mM DTT, 1 mM benzamidine, 10-B-glycerophosphate, 10 mg/ml aprotinin, 10 mg/ml leupeptin, 1 mg/ml pepstatin A, and 1% phosphatase inhibitor cocktail 1. The cell lysates were collected and sonicated for 5 min. Each sample was centrifuged at 12,000 rpm for 10 min at 4°C, after which the supernatant was collected, and protein concentrations were estimated using a bicinchonic acid (BCA) protein assay kit (Pierce, Bonn, Germany).

Cell viability

A standard 3-(4, 5-dimethylthiazol-2-yl)-2, 5-diphenyl tetrazolium bromide (MTT) assay was used as previously described [10]. In brief, MTT was dissolved in isotonic phosphate buffer (pH 7.4) solution at 5 mg/ml and filter-sterilized to remove any insoluble material. MSCs were cultured in DMEM containing 10% FBS until they reached 80% confluence. The cells were then incubated for 4 h at 37°C in serum-free DMEM and cultured as described above. Cells were transfected with 10 nM of control siRNA or specific siRNA IGF-1 and pretreated with or without SAM (10 μM) for 6 h. The absorbance was measured at 570 nm.

Statistical analyses

The statistical significance was evaluated using analysis of variance (ANOVA) and Student's t-test. A probability value of $p<0.05$ was considered to indicate statistical significance.

Results

Characterization of MSCs

MSCs were isolated from bone-marrow cells based on adhesion to tissue culture surfaces. The cell population was heterogeneous with a predominant spindle-shaped morphology and formed fibroblast-like colonies in phase-contrast micrographs. The MSCs in the rat bone marrow cultured for three days and one, two, and three weeks were photographed (Figure 1) and confirmed by fluorescence cell sorting using MSC marker-specific antibodies. MSCs were identified based on the expression of both CD29 and CD90.1 surface markers, as described in our previous report [10].

Effects of SAM on cell viability and endogenous IGF-I

For this study, primary cultured cells from rat bone marrow were used because they can differentiate into various cells types under specific culture conditions. To confirm the effects of SAM on MSC survival, we determined cell viability using the MTT method. Cell viability increased after treatment with SAM in a dose-dependent manner, with a significant increase in response to 10 μM SAM (Figure 2A, $p<0.05$). Subsequently, to confirm whether SAM affected cell viability through IGF-I, we determined the concentrations of endogenous IGF-I mRNA and protein after SAM treatment using RT-PCR and immunoprecipitation Western blotting, respectively. Endogenous IGF-I, which is directly related to cell survival and proliferation, was increased by SAM treatment in a dose-dependent manner (Figures 2B and C). In particular, IGF-I mRNA and protein concentrations significantly increased in response to 1 μM and 10 μM SAM (Figures 2B and C, $p<0.05$ and $p<0.01$, respectively).

Effects of H_2O_2-induced apoptosis on cell viability, ROS generation, and endogenous Nrf2 and IGF-I

To confirm that H_2O_2 treatment induced MSCs to undergo apoptosis, we measured cell viability, ROS production, and Nrf2 and IGF-I mRNA and protein concentrations using Western blotting and quantitative real-time PCR. We confirmed the effects of H_2O_2 on cell viability and ROS production with the MTT and DCFH-DA assays. Treatment with H_2O_2 for 6 h as an oxidant dose-dependently increased ROS generation, with a significant increase at 0.5 and 1 mM (Figure 3A, $p<0.05$ and $p<0.01$, respectively). The cell viability of MSCs treated with H_2O_2 for 6 h decreased with increasing treatment concentration (0.1, 0.5 and 1 mM), with a significant decrease at 1 mM compared to the controls (Figure 3B, $p<0.05$). IGF-I and Nrf2 mRNA and protein concentrations also decreased after treatment with H_2O_2 in a dose-dependent manner. In particular, treatment with 1 mM H_2O_2 decreased the mRNA expression of IGF-I and Nrf2 as compared to the control (Figure 4A, B, C and D, $p<0.05$).

Effects of SAM on cell viability and Nrf2 and IGF-I activity in H_2O_2-induced apoptosis

To investigate whether SAM has a cytoprotective effect against H_2O_2-induced apoptosis, we assessed the cell viability and endogenous IGF-I and Nrf2 levels after co-treatment with 1 mM H_2O_2 and increasing SAM concentrations (0.1, 1, and 10 uM). Treatment of MSCs with 1 mM H_2O_2 for 6 h significantly decreased cell viability as well as IGF-1 and Nrf2 mRNA and protein levels compared to those of the controls (Figure 5A-E, $p<0.01$ and $p<0.05$, respectively). However, the H_2O_2-

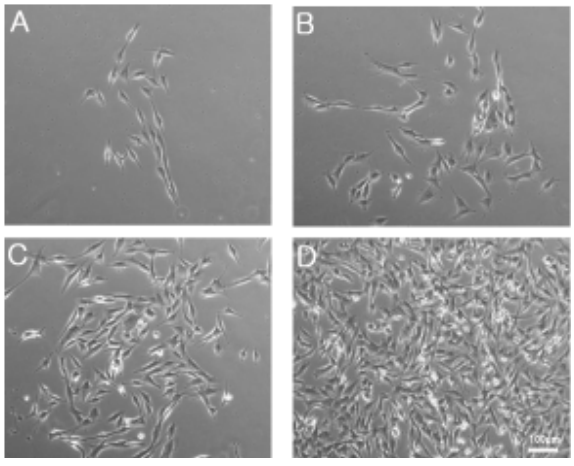

MSCs were isolated from bone marrow at high purity. Cells expressing CD90.1 and CD29 were identified using fluorescence-activated cell sorting. Cells consisted of a heterogeneous cell population with a predominant spindle morphology. Cells cultured for three days (A) and one (B), two (C), and three weeks (D) were photographed, and MSCs proliferated to form a small colony on day 3. A large colony of densely distributed spindle- and triangle-shaped MSCs formed after three weeks.

Figure 1: Phase-contrast micrographs of MSCs at three days and one, two, and three weeks of primary culture.

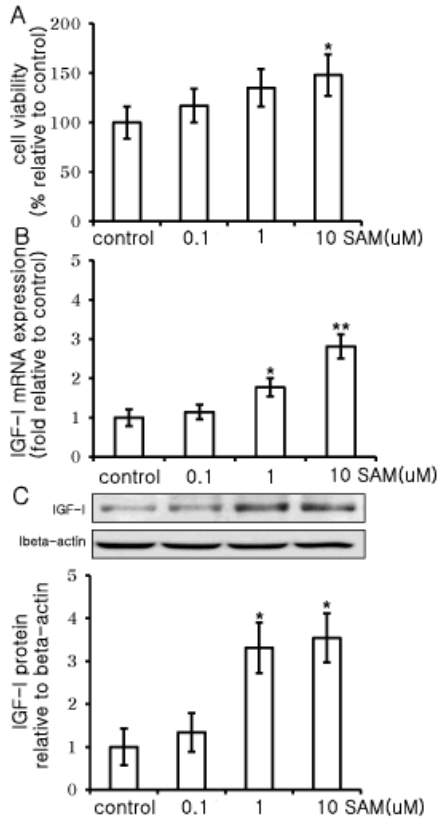

Cells were treated with different concentrations of SAM (0, 0.1, 1 and 10 μM) for 24 h. Cell viability was measured with an MTT assay (A). This expression is expressed as the mean ± SD of the fold- and percent-increases over that of the control. IGF-I mRNA expression was expressed as a fold-increase over that of the control using real-time PCR (B). IGF-1 protein expression was determined using immunoprecipitation and Western blot analysis (C). The mean intensity was measured with densitometry (n=8). Statistical analysis; *p<0.05 and **p<0.05 vs. negative control (control media alone).

Figure 2: Effects of SAM on cell viability and IGF-1 mRNA and protein levels.

induced decreases in cell viability and IGF-1 and Nrf2 mRNA and protein levels were recovered back to control levels by SAM (Figure 5A-E, p<0.01 and p<0.05, respectively). In particular, treatment with 10 μM SAM significantly increased cell viability and IGF-1 and Nrf2 mRNA and protein levels compared to the cells treated with H_2O_2 alone (Figs. 5A, B, C, D and E, p<0.0 and p<0.05, respectively). To demonstrate the cell survival effect of SAM on H_2O_2-induced apoptosis, we used the Annexin-V assay to confirm oxidative stress-induced apoptosis in the positive control after treatment with 1 mM for 6 h (Figure 6).

As shown Figure 6, the control group was not stained with PI or FITC (95.06%), and neither was the group treated with 10 μM SAM alone (97.19%). Treatment with 1 mM H_2O_2 for 6 h resulted in PI and FITC staining (21.89%). Co-treatment with H_2O_2 and SAM reduced staining to near-control levels (89.28%). We also confirmed the cell survival effect of SAM on H_2O_2-induced apoptosis of MSCs using phase-contrast microscopy. This result showed that H_2O_2-induced apoptosis in MSCs was recovered by 10 μM SAM (Figure 7). In the immunofluorescence staining, endogenous Nrf2 activity in the MSCs after 6 h of H_2O_2 treatment decreased more than the control and the cells treated with 10 μM SAM alone, as illustrated in the fluoroscopic photographs (Figure 8 panel A, B and C). Endogenous Nrf2 activity in the controls was similar to those observed after treatment with 10 μM SAM alone (Figure 8 panel A and C). However, the H_2O_2-induced decrease in Nrf2 activity was increased by 10 μM SAM (Figure 8 panel B and D).

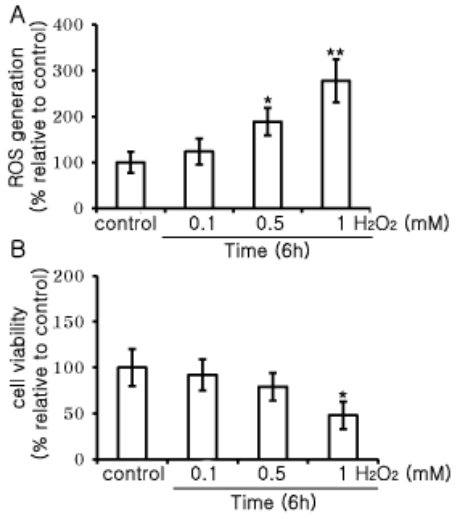

Cells were treated with different concentrations (0, 0.1, 0.5 and 1 mM) of H_2O_2 for 6 h. Cell viability was measured with an MTT assay. Cell viability significantly decreased with increased treatment with 1 mM H2O2 at 6 h (B), and results are expressed as the mean ± SD of fold- and percent-increases over that of the control (n=8). ROS were measured using DCFH-DA (A). The fluorescent intensity was measured at 530 nm after excitation at 490 nm. Fluorescent levels are expressed as percent increase over the control, and are expressed as mean ± SD (n=8). Statistical analysis; *p<0.01, and **p<0.05 vs. negative control (control media alone).

Figure 3: Dose-dependent effects of H_2O_2 on cell viability and ROS generation in MSCs.

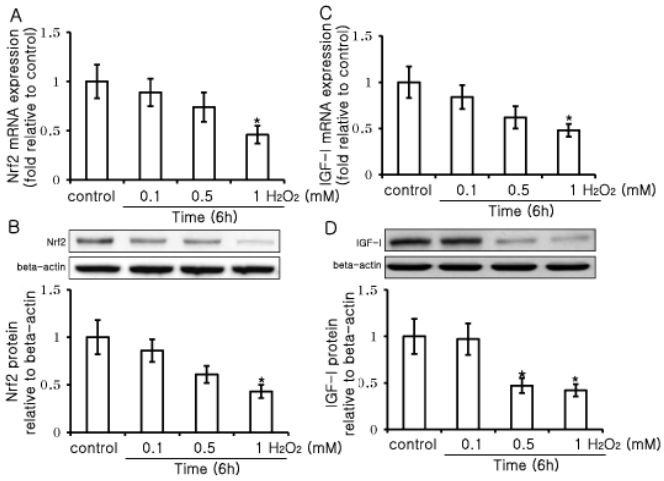

Cells were treated with different concentrations (0, 0.1, 0.5 and 1mM) of H_2O_2 for 6 h. IGF-1 and Nrf2 mRNA expression was measured using real-time PCR (A, C). IGF-1 and Nrf2 proteins were measured using immunoprecipitation and Western blotting (B, D). The mean intensity was measured using densitometry. The mRNA and protein levels decreased treatment with 1 mM H_2O_2 (A, B, C, and D). The mean intensity was measured using densitometry. (n=8). Statistical analysis; *p<0.05 vs. negative control (control media alone).

Figure 4: Dose-dependent effects of H_2O_2 on IGF-1 and Nrf2 mRNA and protein levels in MSCs.

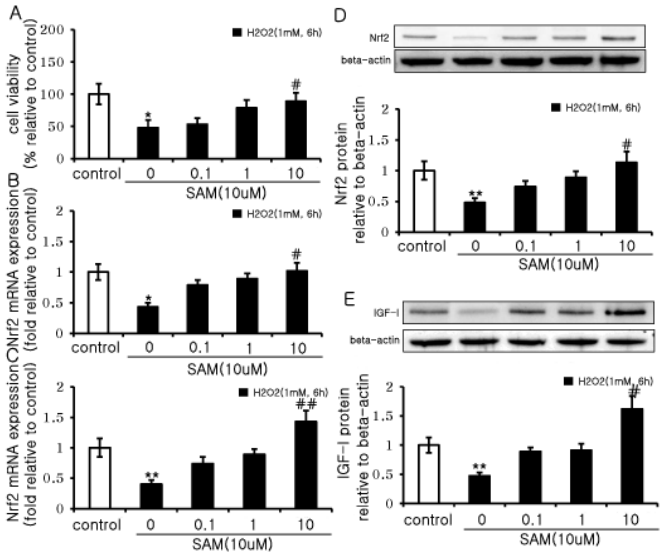

Cells were treated with different concentrations of SAM (0, 0.1, 1 and 10 μM) for 24 h, and then with 1 mM H_2O_2 for 6 h. IGF-1 and Nrf2 mRNA expression was measured using real-time PCR (B, C). IGF-1 and Nrf2 proteins were measured using immunoprecipitation and Western blotting (D, E). The mean intensity was measured using densitometry. SAM reversed the H_2O_2-induced decreases in IGF-I and Nrf2 mRNA and protein levels (B, C, D and E), as well as the decrease in cell viability (A). All expression levels are presented as the mean ± SD of the fold- and percent-increases over that of the control (n=8). Statistical analysis; $^{*}p<0.05$, $^{**}p<0.01$ vs. negative control (control media alone). $^{\#}p<0.05$, $^{\#\#}p<0.01$ vs. positive control (H_2O_2 alone).

Figure 5: Effects of SAM on cell viability and IGF-1 and Nrf2 mRNA and protein expression in H_2O_2-treated MSCs.

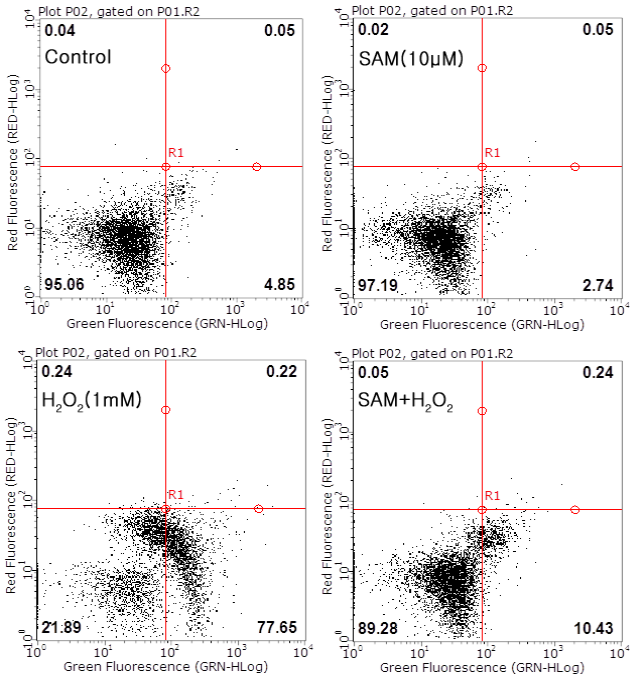

MSCs were treated with 10 μM SAM for 24 h and incubated with 1 mM H_2O_2 for 6 h. H_2O_2–induced apoptosis was recovered by SAM using Annexin V / PI staining.

Figure 6: Flow cytometric analysis indicates anti-apoptotic effects of SAM on H_2O_2-induced oxidative stress.

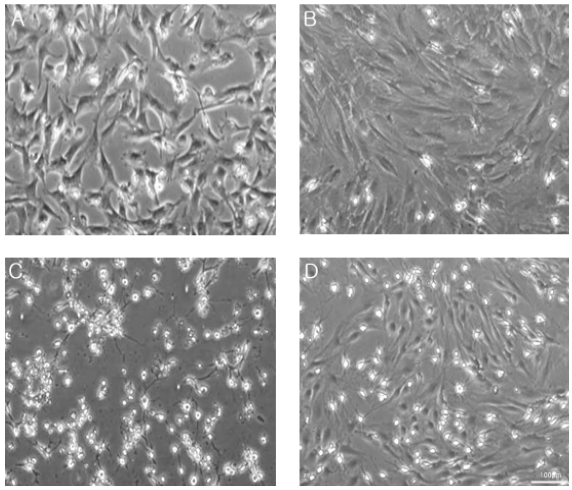

Cells were treated with 10 μM SAM for 24 h, and then with 1 mM H_2O_2 for 6 h. Control (A), SAM 10 μM (B), H_2O_2 for 6 h (C), and co-treatment with SAM and H_2O_2 (D). The effects H_2O_2 treatment on cell morphology and confluency were improved by SAM.

Figure 7: Effects of SAM on H_2O_2-induced apoptosis of MSCs according to phase-contrast microscopy.

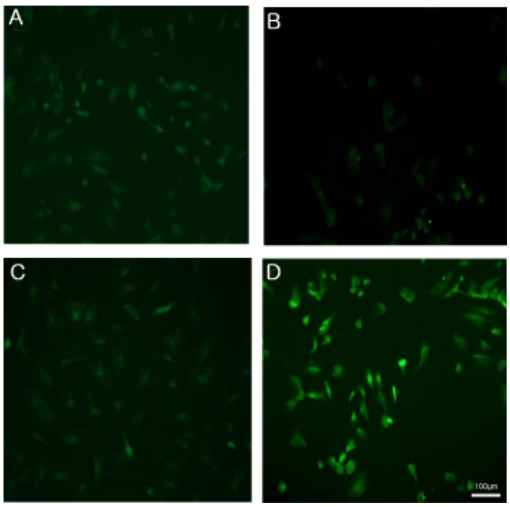

The cellular localization of Nrf2 was determined using immunofluorescence staining with an antibody specific for Nrf2, which was fluorescently labeled using secondary antibodies. Cells were treated with 1 mM H_2O_2 for 6 h. Control (A), H_2O_2 for 6 h (B), SAM (C), and co-treatment with SAM and H_2O_2 (D). Representative microscopy images are shown (green).

Figure 8: Immunocytochemistry analysis indicates the effect of SAM on H_2O_2-induced Nrf2 activation in MSCs.

Relationship between SAM and endogenous Nrf2 and IGF-I in H_2O_2-induced apoptosis

To study the role of IGF-I and Nrf2 on the action of SAM in H_2O_2-induced apoptosis, we first demonstrated successful IGF-I silencing with siRNA transfection. Cells were transfected with siRNA targeting IGF-I and Nrf2 at increasing concentrations (0.1, 1, and 10 nM). Target-specific silencing was determined by comparison of transfection with scrambled siRNA (control siRNA). Treatment with IGF-I and Nrf2 siRNA dose-dependently decreased intercellular Nrf2 and IGF-I

mRNA expression. Silencing was especially effective with 10 nM IGF-I and Nrf2 siRNA as compared to the control (Figure 9A and B). We next confirmed the relationship between SAM-induced regulation of endogenous IGF-I and Nrf2 expression on H_2O_2-induced apoptosis.

Cell viability was inhibited after treatment with H_2O_2 alone compared to the viability of the control, and this decrement was blocked by SAM (Figure 10A). An increase in SAM-induced cell viability in the presence of H_2O_2 was suppressed by treatment with IGF-I and Nrf2 siRNA (Figure 10A, $p<0.05$). On the contrary, the generation of ROS as an indicator of oxidative stress-induced apoptosis increased in cells treated with H_2O_2 alone, and this increase was blocked by SAM (Figure 10B). The decrease in H_2O_2-induced ROS generation with SAM treatment was increased by treatment with IGF-I and Nrf2 siRNA. Endogenous Nrf2 and IGF-I expression was inhibited after treatment with H_2O_2 alone compare to in the control, and this decrement was increased by 10 μM SAM (Figure 11). An increase in SAM-induced endogenous Nrf2 after H_2O_2 treatment was suppressed by IGF-I and Nrf2 siRNA (Figure 11A and B, $p<0.01$ and $p<0.05$, respectively). In particular, IGF-I siRNA reduced the increase in SAM-induced endogenous IGF-I after H_2O_2 treatment, but Nrf2 siRNA was not reduced (Figure 11C and D, $p<0.01$).

To demonstrate the direct relationship of endogenous IGF-I and Nrf2 on exogenous IGF-I-induced cell viability in H_2O_2-induced apoptosis, cells were co-treated with exogenous IGF-I (10-7 M) and Nrf2 siRNA in the presence of H_2O_2. The endogenous IGF-I and Nrf2 also decreased after treatment with H_2O_2 alone compared to the control (Figure 12A-D, $p<0.05$). In the control, the decrease in endogenous Nrf2 and IGF-I expression was recovered back to the baseline after treatment with exogenous IGF-I (Figure 12).

The increase in endogenous Nrf2 after exogenous IGF-I with H_2O_2 treatment was also suppressed by Nrf2 siRNA back to the baseline in the

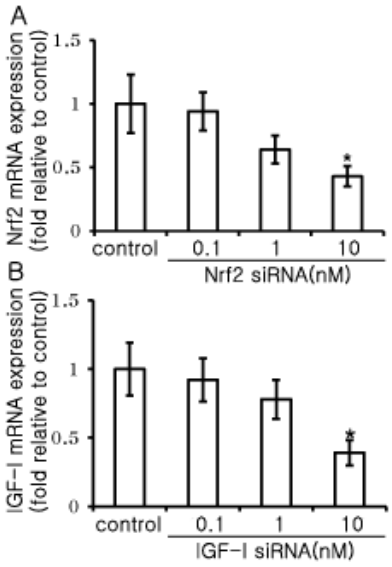

Cells were treated with IGF-I and Nrf2 siRNA at different concentrations (0.1, 1, and 10 nM). The control (control siRNA) is a negative control for RNA interference (A, B). Cells were transfected with IGF-I and Nrf2 siRNA for 24 h. IGF-1 and Nrf2 mRNA expression was measured using real-time PCR. Results are expressed as mean ± SD of fold-increases over that of the control (n=8). Statistical analysis: *p<0.05 vs. negative control (control media).

Figure 9: Effects of IGF-I and Nrf2 siRNA on IGF-I and Nrf2 mRNA levels.

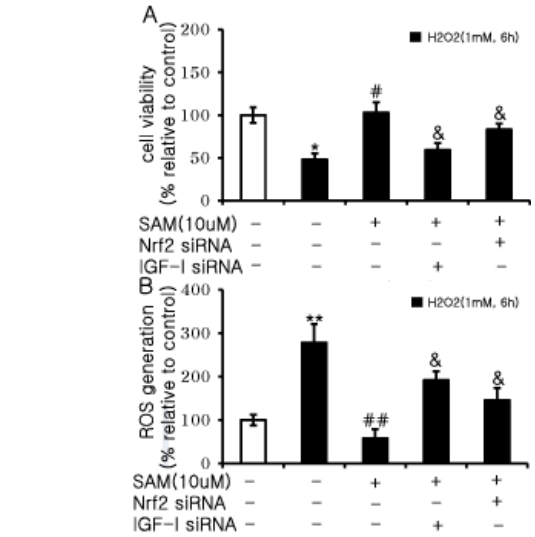

Cells were transfected with specific siRNA and then treated with SAM for 24 h. The cells were post-incubated with 1 mM H_2O_2 for 6 h. The effects of IGF-I and Nrf2 siRNA on SAM-induced cell viability in the presence of H_2O_2 were measured with an MTT assay (A). All expression levels are presented as the percent increase over the control. ROS generation was measured using DCFH-DA (B). The fluorescent intensity was measured at 530 nm after excitation at 490 nm. Fluorescent levels are expressed as the percent increase over the control, and are expressed as mean ± SD (n=8). Statistical analysis; *p<0.01, and **p < 0.05 vs. control media. # p<0.05 and ## p<0.01 vs. media with H_2O_2 alone. & p < 0.05 vs. media with SAM and H_2O_2.

Figure 10: Effects of IGF-I and Nrf2 silencing on SAM-induced cell viability and ROS generation in H_2O_2-induced apoptosis.

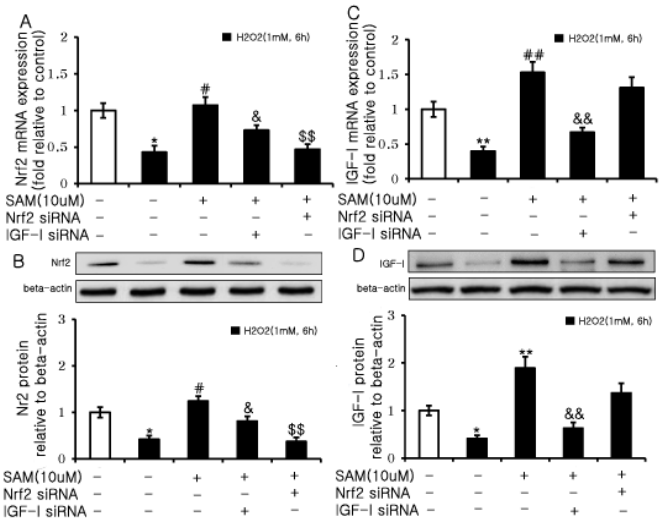

Cells were transfected by specific siRNA and then treated with SAM for 24 h. The cells were post-incubated with 1 mM H_2O_2 for 6h. The effects of IGF-I and Nrf2 siRNA on SAM-induced endogenous IGF-I and Nrf2 in the presence of H_2O_2 was measured using real-time PCR, and IGF-1 and Nrf2 protein levels were measured using immunoprecipitation and Western blotting (A, B, C and D). The mean intensity was measured using densitometry. The results are expressed as mean ± SD of the fold-increases over that of the control (n=8). Statistical analysis: *p<0.01, and **p<0.05 vs. control media. # p<0.05 and ## p<0.01 vs. media with H_2O_2 alone. and p<0.05 and $$ p<0.01 vs. media with SAM and H_2O_2.

Figure 11: Effects of IGF-I and Nrf2 silencing on SAM-induced IGF-I and Nrf2 activity in H_2O_2-induced apoptosis.

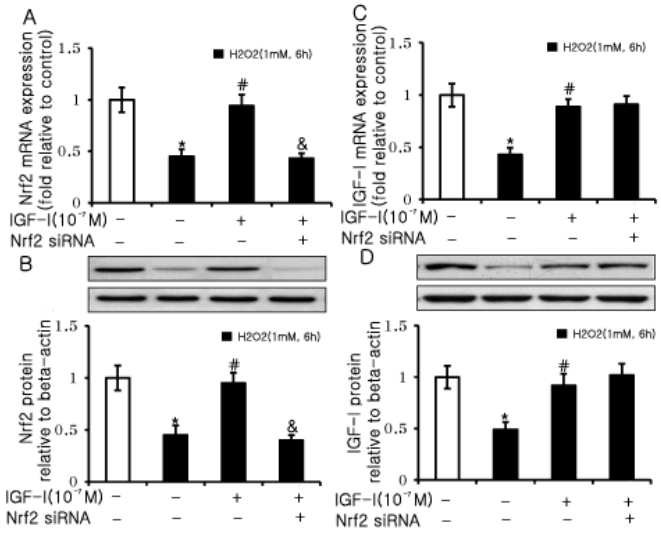

Cells were transfected by Nrf2 siRNA and then treated with exogenous IGF-I for 24 h. The cells were post-treated with 1 mM H_2O_2 for 6 h. The effects of endogenous IGF-I and Nrf2 on exogenous IGF-I and Nrf2 siRNA in the presence of H_2O_2 was measured using real-time PCR, and IGF-1 and Nrf2 protein levels were measured using immunoprecipitation and Western blotting (A, B, C and D). The mean intensity was measured using densitometry. The results are expressed as the mean ± SD of fold-increases over that of the control (n=8). Statistical analysis: *p<0.01, and **p<0.05 vs. control media. # p<0.05 and ## p<0.01 vs. media with IGF-I and H_2O_2. & p<0.05 vs. media with IGF-I and H_2O_2.

Figure 12: Effects of endogenous IGF-I and Nrf2 on exogenous IGF-I and Nrf2 silencing in H_2O_2-induced apoptosis.

cells that received H_2O_2 alone, but endogenous IGF-I was not inhibited (Figure 12A-D, p<0.05). This finding showed that the cytoprotective effect of SAM against oxidative stress-induced apoptosis involves the activation of endogenous IGF-I and Nrf2. Furthermore, the decrease in endogenous Nrf2 activity during oxidative stress was up-regulated by IGF-I in MSCs.

Discussion

Despite the promise of MSCs for repopulating damaged tissue and restoring function in the field of regenerative medicine [32], the poor survival of MSCs following implantation has limited their therapeutic efficacy [33]. The exact cellular mechanisms resulting in MSC loss are unclear [10,11]. The present study demonstrated a cytoprotective effect of SAM on rat MSCs against oxidative stress-induced apoptosis, which was related to its effect on Nrf2 and IGF-I. We first generated a high-purity culture by separating MSCs from rat bone marrow on the basis of binding to CD90.1 and CD29 antibodies [10]. MSC morphologies were consistent with those noted in other studies, consisting of a heterogeneous cell population with a predominantly spindle morphology, with cells forming fibroblast-like colonies [34]. We also confirmed that the MSCs in the rat bone marrow cultured for three days and one, two, and three weeks were photographed, ensuring that the MSC preparations were very pure. Using these primary MSCs, we confirmed that cell viability and endogenous IGF-I levels dose-dependently increased with SAM treatment, with a significant increase in response to 10 μM SAM.

S-Adenosyl-L-methionine (SAM) is a methyl donor that exerts anti-oxidative and cytoprotective effects under various conditions [14-16]. SAM is particularly important for opposing the toxicity of free radicals generated by various toxins [35]. Insulin-like growth factor-I (IGF-I) also plays an important role in bone cell proliferation and oxidative stress-induced apoptosis [17,18]. However, the cytoprotective effect of SAM on oxidative stress-induced apoptosis and the role Nrf2 and IGF-I have not been studied in rat MSCs, despite their potential to differentiate into endothelial cells, fibroblasts, adipocytes, and osteogenic cells. Our results suggest that SAM affects cell viability and endogenous IGF-I levels, which are directly related to cell survival and proliferation in rat MSCs.

Various mechanisms have been implicated in MSC survival, including the transduction of oxidative stress. The ROS-mediated mechanism is one of the earliest-discovered and most important cellular responses to many protective and oxidative stress-induced signaling pathways [36]. Nrf2 overexpression in MSCs has been reported to reduce oxidative stress-induced apoptosis and cytotoxicity [11]. Nrf2 signaling might up-regulate certain anti-apoptotic genes [37-40]. Activated Nrf2 impairs liver regeneration in mice by activating genes involved in cell-cycle control and apoptosis [27]. Although the protective and anti-oxidative effects of SAM are already known, the roles of Nrf2 and IGF-I in the cytoprotective effects of SAM against oxidative stress are not yet clear.

To demonstrate the effects of SAM on cell viability and endogenous IGF-I and Nrf2 activity in oxidative stress-induced cell apoptosis, we first treated MSCs with increasing concentrations of H_2O_2 for 6 h. This treatment dose-dependently decreased cell viability and endogenous IGF-I and Nrf2 levels, with significant decreases after treatment with 1 mM H_2O_2 for 6 h and increased ROS generation. Cell viability and endogenous IGF-I and Nrf2 levels in the MSCs temporarily increased, and then at 6 h decreased after treatment with H_2O_2 (no data). This temporarily increase in Nrf2 was consistent with the findings of a previous report suggesting that transient H_2O_2 treatment temporarily induced a rapid accumulation of Nrf2 protein [24]. These results suggest that short exposures to H_2O_2 increases endogenous Nrf2 and IGF-1 levels due to cellular responses to oxidative stress. However, H_2O_2 treatment for 6 h decreased endogenous Nrf2 and IGF-I levels because it induced apoptosis. The role of H_2O_2 concentration in oxidative stress-induced apoptosis and its impact on cell viability and ROS generation was confirmed at 1mM. Furthermore, the concentration of hydrogen peroxide needed for oxidative stress differed based on the study because it is dependent on the culturing conditions of the MSCs [11,41].

We examined the effects of a 6 h treatment with 1 mM H_2O_2 and SAM on cell viability as well as the endogenous IGF-I and Nrf2 levels after oxidative stress-induced apoptosis. Decreases in H_2O_2-induced cell viability, and Nrf2 and IGF-I levels were recovered by SAM. An Annexin V assay demonstrated that H_2O_2 treatment induced MSC apoptosis, consistent with oxidative stress-induced apoptosis and cytotoxicity [11], although this was also recovered by SAM. Immunocytochemistry confirmed that Nrf2 was inactivated by H_2O_2 treatment and was recovery by SAM. These results suggested that SAM not only increased cell viability, but also increased endogenous Nrf2 and IGF-I levels during oxidative stress-induced apoptosis. These collective observations suggest that SAM increases resistance to oxidative stress and improves cell viability by producing endogenous IGF-I and Nrf2 in murine MSCs.

In the current study, we used IGF-I and Nrf2 siRNA to investigate the roles of Nrf2 and IGF-I on the action of SAM against oxidative stress-induced apoptosis. The increases in SAM-induced cell viability and endogenous IGF-I expression in the presence of H_2O_2 were suppressed by treatment with IGF-I siRNA, but was not blocked by Nrf2 siRNA.

However, the decrease in SAM-induced endogenous Nrf2 was blocked by IGF-I siRNA; this suggests that endogenous IGF-I is more important than endogenous Nrf2 in cell survival against oxidative stress-induced apoptosis. These results indicate that the cytoprotective effect of SAM on oxidative stress-induced apoptosis increased endogenous Nrf2 and IGF-I activity, and increases in Nrf2 activity protected cells via IGF-I in rat bone marrow mesenchymal stem cells.

To demonstrate the direct relationship of endogenous IGF-I and Nrf2 with SAM-mediated cell viability in H_2O_2-induced apoptosis, cells were co-treated with exogenous IGF-I and Nrf2 siRNA in the presence of H_2O_2. Nrf2 siRNA in the presence of H_2O_2, suppressed increases in endogenous Nrf2 mediated by exogenous IGF-I to the baseline levels of cells treated with H_2O_2 alone; Nrf2 siRNA did not change endogenous IGF-I levels. We further showed that the cytoprotective effect of SAM against oxidative stress-induced apoptosis was related to endogenous IGF-I and Nrf2 activation, and that decreases in Nrf2 activity in conditions of oxidative stress-induced apoptosis were up-regulated by IGF-I in rat bone marrow mesenchymal stem cells.

Nrf2, an anti-oxidative transcription factor, translocates to the nucleus and binds ARE in response to oxidative stress [42,43]. The cellular mechanism of Nrf2 activity is regulated by phosphorylation by PI3 and extracellular signals regulated by kinases [44,45]. Hsp20-engineered mesenchymal stem cells are resistant to oxidative stress via the enhanced activation of Akt and the increased secretion of growth factors [46]. IGF-1 also increases MSC migratory responses though a PI3/Akt-dependent mechanism [47]. Our previous study reported that short-term treatment with PTH had a protective effect against oxidative stress by affecting endogenous IGF-I and Nrf2 levels in rat bone marrow-derived mesenchymal cells [10]. This result implies that the cytoprotective effects of SAM on H_2O_2-induced apoptosis are mediated by increasing Nrf2 levels, consistent with the observation that IGF-I promotes PI3/Akt phosphorylation; toward this point, Nrf2 and IGF-I expression have been assessed in benign, premalignant, and malignant gastric lesions [48,49].

Taken together, these findings indicate that oxidative stress-induced apoptosis in MSCs decreases cell viability and endogenous Nrf2 and IGF-I levels, and that these negative effects are recovered by SAM. Furthermore, this evidence indicates that the cytoprotective effect of SAM occurs by increasing endogenous Nrf2 activity through IGF-I.

Clinically, Nrf2 overexpression induced by SAM could be used to prevent the death of transplanted graft cells, thus improving MSC resistance to oxidative and apoptotic stimuli.

Acknowledgements

This paper was supported by research funds from Chonbuk National University in 2014.

References

1. Kassem M, Abdallah BM, Saeed H (2008) Osteoblastic cells: differentiation and trans-differentiation. Arch Biochem Biophys 473: 183-187. [PubMed]
2. Chen LB, Jiang XB, Yang L Differentiation of rat marrow mesenchymal stem cells into pancreatic islet beta-cells. World J Gastroenterol 10: 3016-3020. [PubMed]
3. Franchini M (2003) Mesenchymal stem cells: from biology to clinical applications. Recenti Prog Med 94: 478-483. [PubMed]
4. Dominici M, Le Blanc K, Mueller I, Slaper-Cortenbach I, Marini F, et.al. (2006) Minimal criteria for defining multipotent mesenchymal stromal cells. The International Society for Cellular Therapy position statement. Cytotherapy 8: 315-317. [PubMed]
5. Zhang W, Su X, Gao Y, Sun B, Yu Y, et.al. (2009) Berberine protects mesenchymal stem cells against hypoxia-induced apoptosis in vitro. Biol Pharm Bull 32: 1335-1342. [PubMed]
6. Iwase T, Nagaya N, Fujii T, Itoh T, Murakami S, et.al. (2005) Comparison of angiogenic potency between mesenchymal stem cells and mononuclear cells in a rat model of hindlimb ischemia. Cardiovasc Res 66: 543-551. [PubMed]
7. Toma C, Pittenger MF, Cahill KS, Byrne BJ, Kessler PD (2002) Human mesenchymal stem cells differentiate to a cardiomyocyte phenotype in the adult murine heart. Circulation 105: 93-98. [PubMed]
8. Zhang M, Methot D, Poppa V, Fujio Y, Walsh K, et.al. (2001) Cardiomyocyte grafting for cardiac repair: graft cell death and anti-death strategies. J Mol Cell Cardiol 33: 907-921. [PubMed]
9. Jung TW, Lee JY, Shim WS, Kang ES, Kim SK, et.al. (2007) Rosiglitazone protects human neuroblastoma SH-SY5Y cells against MPP+ induced cytotoxicity via inhibition of mitochondrial dysfunction and ROS production. J Neurol Sci 253: 53-60. [PubMed]
10. Oh YI, Kim JH, Kang CW (2014) Protective effect of short-term treatment with parathyroid hormone 1-34 on oxidative stress is involved in insulin-like growth factor-I and nuclear factor erythroid 2-related factor 2 in rat bone marrow derived mesenchymal stem cells. Regul Pept 189: 1-10. [PubMed]
11. Mohammadzadeh M, Halabian R, Gharehbaghian A, Amirizadeh N, Jahanian-Najafabadi A, et.al. (2012) Nrf-2 overexpression in mesenchymal stem cells reduces oxidative stress-induced apoptosis and cytotoxicity. Cell Stress Chaperones 17: 553-565. [PubMed]
12. Cantoni GL (1975) Biological methylation: selected aspects. Annu Rev Biochem 44: 435-451. [PubMed]
13. Mato JM, Alvarez L, Ortiz P, Pajares MA (1997) S-adenosylmethionine synthesis: molecular mechanisms and clinical implications. Pharmacol Ther 73: 265-280. [PubMed]
14. Cederbaum AI (2010) Hepatoprotective effects of S-adenosyl-L-methionine against alcohol- and cytochrome P450 2E1-induced liver injury. World J Gastroenterol 16: 1366-1376. [PubMed]
15. Laudanno OM (1987) Cytoprotective effect of S-adenosylmethionine compared with that of misoprostol against ethanol-, aspirin-, and stress-induced gastric damage. Am J Med 83: 43-47. [PubMed]
16. Chang CY, Argo CK, Al-Osaimi AM, Caldwell SH (2006) Therapy of NAFLD: antioxidants and cytoprotective agents. J Clin Gastroenterol 40: S51-60. [PubMed]
17. Mohan S, Baylink DJ (1993) Characterization of the IGF regulatory system in bone. Adv Exp Med Biol 343: 397-406. [PubMed]
18. Linkhart TA, Mohan S, Baylink DJ (1996) Growth factors for bone growth and repair: IGF, TGF beta and BMP. Bone 19: 1S-12S. [PubMed]
19. Benito M, Valverde AM, Lorenzo M (1996) IGF-I: a mitogen also involved in differentiation processes in mammalian cells. Int J Biochem Cell Biol 28: 499-510. [PubMed]
20. Rabkin R, Schaefer F (2004) New concepts: growth hormone, insulin-like growth factor-I and the kidney. Growth Horm IGF Res 14: 270-276. [PubMed]
21. Buckley BJ, Marshall ZM, Whorton AR (2003) Nitric oxide stimulates Nrf2 nuclear translocation in vascular endothelium. Biochem Biophys Res Commun 307: 973-979. [PubMed]
22. Nguyen T, Sherratt PJ, Pickett CB (2003) Regulatory mechanisms controlling gene expression mediated by the antioxidant response element. Annu Rev Pharmacol Toxicol 43: 233-260. [PubMed]
23. Jaiswal AK (2004) Nrf2 signaling in coordinated activation of antioxidant gene expression. Free Radic Biol Med 36: 1199-1207. [PubMed]
24. Purdom-Dickinson SE, Sheveleva EV, Sun H, Chen QM (2007) Translational control of nrf2 protein in activation of antioxidant response by oxidants. Mol Pharmacol 72: 1074-1081. [PubMed]
25. Zhu H, Zhang L, Itoh K, Yamamoto M, Ross D, et.al. (2006) Nrf2 controls bone marrow stromal cell susceptibility to oxidative and electrophilic stress. Free Radic Biol Med 41: 132-143. [PubMed]
26. Huang HC, Nguyen T, Pickett CB (2000) Regulation of the antioxidant response element by protein kinase C-mediated phosphorylation of NF-E2-related factor 2. Proc Natl Acad Sci U S A 97: 12475-12480. [PubMed]

27. Kohler UA, Kurinna S, Schwitter D, Marti A, Schafer M, et.al. (2014) Activated Nrf2 impairs liver regeneration in mice by activation of genes involved in cell-cycle control and apoptosis. Hepatology 60: 670-678. [PubMed]

28. Lee JM, Calkins MJ, Chan K, Kan YW, Johnson JA (2003) Identification of the NF-E2-related factor-2-dependent genes conferring protection against oxidative stress in primary cortical astrocytes using oligonucleotide microarray analysis. J Biol Chem 278: 12029-12038. [PubMed]

29. Rzhaninova AA, Gornostaeva SN, Goldshtein DV (2005) Isolation and phenotypical characterization of mesenchymal stem cells from human fetal thymus. Bull Exp Biol Med 139: 134-140. [PubMed]

30. Jarocha D, Lukasiewicz E, Majka M (2008) Adventage of mesenchymal stem cells (MSC) expansion directly from purified bone marrow CD105+ and CD271+ cells. Folia Histochem Cytobiol 46: 307-314. [PubMed]

31. Robinson JP (2001) Oxidative metabolism, John Wiley and Sons, Inc. Curr Protoc Cytom Chapter 9: Unit 9.7. [PubMed]

32. Zhu W, Chen J, Cong X, Hu S, Chen X (2006) Hypoxia and serum deprivation-induced apoptosis in mesenchymal stem cells. Stem Cells 24: 416-425. [PubMed]

33. Li W, Ma N, Ong LL, Nesselmann C, Klopsch C, et.al. (2007) Bcl-2 engineered MSCs inhibited apoptosis and improved heart function. Stem Cells 25: 2118-2127. [PubMed]

34. Liu Y, Song J, Liu W, Wan Y, Chen X, et.al. (2003) Growth and differentiation of rat bone marrow stromal cells: does 5-azacytidine trigger their cardiomyogenic differentiation? Cardiovasc Res 58: 460-468. [PubMed]

35. Avila MA, Garcia-Trevijano ER, Martinez-Chantar ML, Latasa MU, Perez-Mato I, et.al. (2002) S-Adenosylmethionine revisited: its essential role in the regulation of liver function. Alcohol 2002, 27: 163-167. [PubMed]

36. Poli G, Leonarduzzi G, Biasi F, Chiarpotto E (2004) Oxidative stress and cell signalling. Curr Med Chem 11: 1163-1182. [PubMed]

37. Levonen AL, Inkala M, Heikura T, Jauhiainen S, Jyrkkanen HK, et.al. (2007) Nrf2 gene transfer induces antioxidant enzymes and suppresses smooth muscle cell growth in vitro and reduces oxidative stress in rabbit aorta in vivo. Arterioscler Thromb Vasc Biol 27: 741-747. [PubMed]

38. Ho HK, White CC, Fernandez C, Fausto N, Kavanagh TJ, et.al. (2005) Nrf2 activation involves an oxidative-stress independent pathway in tetrafluoroethylcysteine-induced cytotoxicity. Toxicol Sci 86: 354-364. [PubMed]

39. Calkins MJ, Johnson DA, Townsend JA, Vargas MR, Dowell JA, et.al. (2009) The Nrf2/ARE pathway as a potential therapeutic target in neurodegenerative disease. Antioxid Redox Signal 11: 497-508. [PubMed]

40. Nakaso K, Yano H, Fukuhara Y, Takeshima T, Wada-Isoe K, et.al. (2003) PI3K is a key molecule in the Nrf2-mediated regulation of antioxidative proteins by hemin in human neuroblastoma cells. FEBS Lett 546: 181-184. [PubMed]

41. Wang FW, Wang Z, Zhang YM, Du ZX, Zhang XL, et.al. (2013) Protective effect of melatonin on bone marrow mesenchymal stem cells against hydrogen peroxide-induced apoptosis in vitro. J Cell Biochem 114: 2346-2355. [PubMed]

42. Kang KW, Lee SJ, Kim SG (2005) Molecular mechanism of nrf2 activation by oxidative stress. Antioxid Redox Signal 7: 1664-1673. [PubMed]

43. Rhee SG, Yang KS, Kang SW, Woo HA, Chang TS (2005) Controlled elimination of intracellular H(2)O(2): regulation of peroxiredoxin, catalase, and glutathione peroxidase via post-translational modification. Antioxid Redox Signal 7: 619-626. [PubMed]

44. Zhang H, Liu H, Iles KE, Liu RM, Postlethwait EM, et.al. (2006) 4-Hydroxynonenal induces rat gamma-glutamyl transpeptidase through mitogen-activated protein kinase-mediated electrophile response element/nuclear factor erythroid 2-related factor 2 signaling. Am J Respir Cell Mol Biol 34: 174-181. [PubMed]

45. Kang KW, Ryu JH, Kim SG (2000) The essential role of phosphatidylinositol 3-kinase and of p38 mitogen-activated protein kinase activation in the antioxidant response element-mediated rGSTA2 induction by decreased glutathione in H4IIE hepatoma cells. Mol Pharmacol 58: 1017-1025. [PubMed]

46. Wang X, Zhao T, Huang W, Wang T, Qian J, et.al. (2009) Hsp20-engineered mesenchymal stem cells are resistant to oxidative stress via enhanced activation of Akt and increased secretion of growth factors. Stem Cells 27: 3021-3031. [PubMed]

47. Li Y, Yu X, Lin S, Li X, Zhang S, et.al. (2007) Insulin-like growth factor 1 enhances the migratory capacity of mesenchymal stem cells. Biochem Biophys Res Commun 356: 780-784. [PubMed]

48. Ribeiro M, Rosenstock TR, Oliveira AM, Oliveira CR, Rego AC (2014) Insulin and IGF-1 improve mitochondrial function in a PI-3K/Akt-dependent manner and reduce mitochondrial generation of reactive oxygen species in Huntington's disease knock-in striatal cells. Free Radic Biol Med 74: 129-144. [PubMed]

49. Wang HB, Zhou CJ, Song SZ, Chen P, Xu WH, et.al. (2011) Evaluation of Nrf2 and IGF-1 expression in benign, premalignant and malignant gastric lesions. Pathol Res Pract 207: 169-173. [PubMed]